Am. J. Hum. Genet. 73:174–187, 2003

Loss of Kindlin-1, a Human Homolog of the *Caenorhabditis elegans* Actin–Extracellular-Matrix Linker Protein UNC-112, Causes Kindler Syndrome

Dawn H. Siegel,[1,*] Gabrielle H. S. Ashton,[2,*] Homero G. Penagos,[4] James V. Lee,[5] Heidi S. Feiler,[5] Kirk C. Wilhelmsen,[5] Andrew P. South,[2] Frances J. D. Smith,[6] Alan R. Prescott,[7] Vesarat Wessagowit,[2] Noritaka Oyama,[2] Masashi Akiyama,[8] Daifullah Al Aboud,[10] Khalid Al Aboud,[11] Ahmad Al Githami,[12] Khalid Al Hawsawi,[11] Abla Al Ismaily,[13] Raouf Al-Suwaid,[13] David J. Atherton,[3] Ruggero Caputo,[14] Jo-David Fine,[15] Ilona J. Frieden,[1] Elaine Fuchs,[16] Richard M. Haber,[17] Takashi Harada,[18] Yasuo Kitajima,[20] Susan B. Mallory,[21] Hideoki Ogawa,[19] Sedef Sahin,[22] Hiroshi Shimizu,[8] Yasushi Suga,[19] Gianluca Tadini,[14] Kikuo Tsuchiya,[9] Colin B. Wiebe,[23] Fenella Wojnarowska,[24] Adel B. Zaghloul,[25] Takahiro Hamada,[2] Rajeev Mallipeddi,[2] Robin A. J. Eady,[2] W. H. Irwin McLean,[6] John A. McGrath,[2] and Ervin H. Epstein, Jr.[1]

[1]Department of Dermatology, San Francisco General Hospital, University of California, San Francisco; [2]Department of Cell and Molecular Pathology, St John's Institute of Dermatology, The Guy's, King's College and St Thomas' Hospitals' Medical School, St Thomas' Hospital, and [3]Department of Dermatology, The Hospital for Sick Children, London; [4]Department of Dermatology, Social Security Bureau of Panama, David, Chiriqui, Panama; [5]Ernest Gallo Clinic and Research Center, Department of Neurology, University of California, Emeryville; [6]Epithelial Genetics Group, Human Genetics Unit, University of Dundee, Ninewells Hospital and Medical School, and [7]Centre for High Resolution Imaging and Processing, School of Life Sciences Biocentre, University of Dundee, Dundee, United Kingdom; [8]Department of Dermatology, Hokkaido University School of Medicine, and [9]Department of Dermatology, Sapporo City Hospital, Sapporo; [10]King Faisal Specialist Hospital and Research Center, Riyadh; [11]Department of Dermatology, King Faisal Hospital, Taif, Saudi Arabia; [12]King Khalid National Guard Hospital, Jeddah, Saudi Arabia; [13]Department of Dermatology, Al Nahdha Hospital, Ruwi, Oman; [14]Department of Dermatology, Center for Inherited Cutaneous Diseases, Institute of Dermatological Sciences, University of Milan, Instituto di Ricovero e Cura a Carattere Scientifico Ospedale Maggiore Policlinico, Milan; [15]Department of Dermatology, University of Kentucky College of Medicine, National Epidermolysis Bullosa Registry, Dermatology Associates of Kentucky, Lexington; [16]Mammalian Cell Biology & Development, Rockefeller University, Howard Hughes Medical Institute, New York; [17]Victoria, British Columbia; [18]Department of Dermatology, Daini Hospital, Tokyo Women's Medical School, and [19]Department of Dermatology, Juntendo University School of Medicine, Tokyo; [20]Department of Dermatology, Gifu University School of Medicine, Gifu, Japan; [21]Washington University School of Medicine, Division of Dermatology, St. Louis, Missouri; [22]Department of Dermatology, Hacettepe University School of Medicine, Ankara; [23]Oral Biological and Medical Sciences, University of British Columbia, Vancouver; [24]Department of Dermatology, Churchill Hospital, Headington, Oxford, United Kingdom; and [25]Cairo Skin V.D. Hospital, El Haud El Marsoud, Cairo

Kindler syndrome is an autosomal recessive disorder characterized by neonatal blistering, sun sensitivity, atrophy, abnormal pigmentation, and fragility of the skin. Linkage and homozygosity analysis in an isolated Panamanian cohort and in additional inbred families mapped the gene to 20p12.3. Loss-of-function mutations were identified in the *FLJ20116* gene (renamed "*KIND1*" [encoding kindlin-1]). Kindlin-1 is a human homolog of the *Caenorhabditis elegans* protein UNC-112, a membrane-associated structural/signaling protein that has been implicated in linking the actin cytoskeleton to the extracellular matrix (ECM). Thus, Kindler syndrome is, to our knowledge, the first skin fragility disorder caused by a defect in actin-ECM linkage, rather than keratin-ECM linkage.

Introduction

In 1954, Theresa Kindler described a 14-year-old English girl with unusual congenital blistering of her hands and feet (Kindler 1954). Later in childhood, the patient developed reticulate erythema and diffuse cutaneous atrophy, beginning in sun-exposed areas. Her gums bled readily, and the skin of the dorsa on her hands and feet had a thin, wrinkled appearance. She also had webbing between the second and third toes on both feet. By 10 years of age, the blistering and sun sensitivity had resolved, but the skin remained thin and fragile.

Thus far, the genetic basis of Kindler syndrome (MIM 173650) has not been delineated. Clinically, it resembles both inherited blistering skin disorders such as dystrophic epidermolysis bullosa (MIM 226600) and congenital poikilodermas such as Rothmund-Thomson

Received April 3, 2003; accepted for publication April 29, 2003; electronically published June 3, 2003.

* The first two authors contributed equally to this work.

0002-9297/2003/7301-0016$15.00

Address for correspondence and reprints: Dr. Ervin Epstein, Jr., San Francisco General Hospital, Building 100, Room 269, 1001 Potrero Avenue, San Francisco, California, 94110. E-mail: ehepstein@orca.ucsf.edu; Dr. John McGrath, St Thomas' Hospital, Lambeth Palace Road, London SE1 7EH, United Kingdom. E-mail: john.mcgrath@kcl.ac.uk; or Dr. Irwin McLean, Epithelial Genetics Group, Human Genetics Unit, Ninewells Hospital and Medical School, Dundee DD1 9SY, United Kingdom. E-mail: wmclean@hgmp.mrc.ac.uk

syndrome (MIM 268400). Although Kindler syndrome is rare, with <100 cases reported in the world literature, we have identified a group of 26 Native American patients with Kindler syndrome who are members of the Ngöbe-Buglé tribe in the Bocas del Toro province, on the northwestern Caribbean coast of Panama. This corresponds to an incidence of ~21/100,000 in this province, which has a population mostly of indigenous people living in small, isolated villages. In the present study, we have localized the gene responsible for Kindler syndrome to 20p12.3, by genomewide linkage analysis in the affected Panamanian subjects. We then confirmed the locus in individuals with Kindler syndrome from diverse geographic backgrounds, some of whom have been described previously (Wiebe et al. 1996; Shimizu et al. 1997; Senturk et al. 1999; Suga et al. 2000; Al Aboud et al. 2002). We have identified loss-of-function mutations in the causative gene, *KIND1*. Kindlin-1 protein is expressed in the epidermis, and in vitro it colocalizes with actin and vinculin in focal contacts. Here, we report an actin–extracellular-matrix (ECM) linkage protein deficiency causing an inherited skin fragility and photosensitivity syndrome.

Subjects and Methods

Affected Individuals

All affected individuals were referred to the present study by their primary dermatologists. Blood samples were obtained after informed consent from members of 24 families from Panama, the United States, Britain, Italy, Oman, Jordan, Turkey, Saudi Arabia, Afghanistan, Pakistan, and Japan, with the approval of the institutional review board at the University of California, San Francisco, and the Ethics Committee at St Thomas' Hospital, London.

Genomewide Screen and Genetic Linkage Analysis

DNA was isolated from whole blood by using a commercial kit (Gentra). Genotypes were generated for a panel of 811 microsatellite dinucleotide markers (Weber and May 1989) by using fluorescently labeled PCR primers, under conditions recommended by the manufacturer (HD5, version 2.0; Applied Biosystems). The sizes of the PCR products for the markers were determined from electropherograms produced with an ABI 3700 DNA sequencer. The sizes of marker amplimers were determined blind to pedigree structure and diagnosis, using Genotyper (ABI). The sex-averaged marker map order was obtained from ABI, from Généthon, or by interpolation of the genomic sequence (see the UCSC Genome Bioinformatics Web site), assuming a uniform marker to physical distance map.

The program PedCheck was used to detect non-Mendelian inheritance (O'Connell and Weeks 1998). Two-point LOD scores were calculated using Vitesse (O'Connell and Weeks 1995). The subjects were genotyped for additional simple-sequence repeat markers from the linked region that were either from Research Genetics or were developed from genomic sequence data. These were evaluated for conserved haplotypes. Multipoint LOD scores were calculated for families in which there were at least two individuals affected or in which there was a known history of consanguinity, using Simwalk2 (Sobel and Lange 1996).

Cell Culture and RNA Extraction

Skin-biopsy samples for keratinocyte culture were subjected to dispase (Sigma-Aldrich) digestion in Dulbecco's PBS (Gibco BRL), to separate the epidermis from the dermis, as described elsewhere (Bleck et al. 1999). Keratinocytes were isolated from the epidermis by incubation in 0.5% trypsin (Invitrogen) at 37°C for 10 min. These cells were plated with a mitomycin C (Sigma-Aldrich)–treated 3T3 feeder layer in keratinocyte growth medium, as described elsewhere (Navsaria et al. 1994). Total RNA was extracted from cultured keratinocytes by using the Qiagen RNeasy Kit (Qiagen). Total RNA quality was checked on a 1% agarose gel in 1 × morphopropane sulfonic acid buffer, to view the ribosomal subunits, 60s and 40s.

cDNA Synthesis

RT-PCR of control RNA was performed in two identical reactions each comprising 2.5 μg total RNA, 4 μl of 10 mM dNTPs, and 2 μl of 50 μM first-strand random primers with the addition of nuclease-free water to make a total of 16 μl, followed by denaturation at 85°C for 3 min in a thermal cycler. Samples were placed on ice, and 2 μl of 10 × RT-PCR buffer and 1 μl of RNasin (Promega) were added. To one sample, 100 U of M-MuLV reverse transcriptase (Promega) was added, and, to the other, 0.5 μl of water was added as a negative control. Samples were incubated in a thermal cycler at 42°C for 1 h, and cDNA was then stored at −20°C.

Multiple-Tissue Northern Blot

A 583-bp cDNA probe of the last 457 bp of the *KIND1* ORF and the first 126 bp of the 3′ UTR was generated from control keratinocyte cDNA. The primers cDNA2F, 5′-ACACAAATCCAAACAGCTGGCC-3′, and cDNA2R, 5′-GTGACCAGCGGTGAATGTAT-3′, were used under standard PCR conditions (described below, in the "Multiple-Tissue cDNA Panels" subsection), at an annealing temperature of 62°C. The forward primer cDNA2F crosses the splice site between exons 12 and 13 of *KIND1* and therefore is cDNA specific. Fifty microliters of probe was loaded on a 2% agarose gel against a 1-kb DNA ladder of known concentration (New England Biolabs UK) and

was gel purified with Prep-A-Gene (Bio-Rad), ready for radiolabeling. Twenty-five nanograms of probe was radiolabeled by random priming (Invitrogen) with [^{32}P]-labeled α-dCTP and was purified using the QIAquick Nucleotide Removal Kit (Qiagen). A multiple-tissue northern blot (Clontech) was hybridized in ExpressHyb solution (Clontech) with 1–2 × 10^6 cpm/ml of labeled probe, followed by washing, according to manufacturer's instructions. In addition, a northern blot was made using total RNA extracted from control keratinocytes, blotted overnight onto a nitrocellulose membrane, and then hybridized in Church solution with 1–2 × 10^6 cpm/ml of labeled probe, followed by washing in Church wash, as described elsewhere (Church et al. 1994). Both blots were subsequently stripped and hybridized with a control human β-actin probe (Clontech), to ensure that the RNA signal intensity was the same in each lane.

Multiple-Tissue cDNA Panels

Primer pairs were designed to amplify cDNA fragments for *KIND1, KIND2,* and *KIND3.* Clontech human normalized multiple-tissue cDNA panels MTCI and -II, in addition to cDNA from control keratinocyte and fibroblast cultures, were amplified by RT-PCR. RT-PCR was performed in duplicate for the housekeeping gene, *G3PDH* (Clontech), to ensure consistent normalization. Negative cDNA controls from keratinocytes and fibroblasts were included and were synthesized as described above (see the "Multiple-Tissue Northern Blot" subsection). PCRs consisting of 5 ng of cDNA as template in a 50-μl reaction containing 0.4 μM of each primer, 1.5 mM of $MgCl_2$, 20 μM of each nucleotide, and 2.5 U of Ampli*Taq* Gold polymerase (PE Biosystems) were cycled at 95°C for 5 min, followed by 95°C for 30 s, 60°C for 30 s, and 72°C for 75 s, for a total of 32 cycles. Aliquots of 5 μl were removed and analyzed after 26, 28, 30, and 32 cycles, enabling the evaluation of tissue-expression levels prior to the PCR plateau phase. The time point for the assessment of expression was set at 30 cycles.

Mutation Detection

Intronic primer pairs were designed to amplify individual exons and flanking splice sites of the *KIND1* gene. Forward and reverse primer sequences are given in table 1. PCR was performed using 250 ng of patient and control genomic DNA as template in a 25-μl reaction that contained 1 μM of each primer, 1.5 mM of $MgCl_2$, 50 μM of each nucleotide, and 1.25 U of *Taq* polymerase (PE Biosystems). Amplification conditions were 95°C for 5 min, followed by 95°C for 45 s, annealing temperature (58°C–60°C) for 45 s, and 72°C for 45 s for 35 cycles in a PE Biosystems 9700 thermal cycler. Five microliters of PCR product was checked on a 2% agarose gel prior to heteroduplex analysis by conformation-sensitive gel electrophoresis, as described elsewhere (Ganguly et al. 1993). PCR products from patients with known consanguinity were mixed with the PCR product amplified from control DNA, to enable heteroduplex formation. Products displaying aberrant band shifts were purified and sequenced using Big Dye Terminator Cycle Sequencing chemistry on an ABI 310 genetic analyzer (PE Biosystems).

Anti-Kindlin-1 Antibody Generation

Anti-rabbit polyclonal antibody was made using the 15 carboxyl-terminal amino acids of kindlin-1, which were cross-linked to keyhole limpet hemocyanin as immunogen (Moravian Biotech). The antiserum was affinity purified against the peptide by using the HiTrap Protein G HP kit (Amersham Biosciences UK), according to the manufacturer's instructions, and was then concentrated using a 10-kDa Microcon-10 concentrator (Amicon).

Immunohistochemistry

Skin was washed in PBS for 30 min before being embedded in OCT compound (Agar Scientific) and was snap frozen in isopentane cooled by liquid nitrogen. Five-micrometer cryosections were fixed in 1:1 acetone and methanol at −20°C for 20 min and were then rehydrated in PBS for 2 × 15 min and incubated in 0.1% Triton-X-100 in PBS prior to blocking with 10% normal goat serum in PBS for 20 min. Sections were then incubated in the same well with primary kindlin-1 rabbit polyclonal antibody at 37°C for 1 h, followed by goat anti-rabbit Alexa Fluor 488 conjugate (Cambridge BioScience) for 1 h. The samples were thoroughly washed in PBS and were subsequently mounted on cover slips. Microscopy was performed using a Nikon Optiphot Microscope with Kodak Microscopy Document System 290.

Kindlin-1 Transfections

A sequence-verified RT-PCR clone in pCR2.1, encompassing the entire kindlin-1 cDNA, was subcloned into pEGFP-C2 (Clontech) for expression of a fusion protein consisting of kindlin-1 fused to the C-terminus of enhanced green fluorescent protein (hereafter, "EGFP-kindlin"). PtK2 cells (potoroo kidney epithelial cell line) were transfected with kindlin constructs using FuGene 6 transfection reagent (Roche Diagnostics). The cells were fixed 24 h posttransfection with 3% paraformaldehyde and were permeabilized using 0.2% Triton X-100 (BDH Chemicals). Fixed cells were stained with Alexa Fluor 594-phalloidin conjugate (1 U/ml) (Molecular Probes) or vinculin mouse monoclonal antibody (Sigma Chemicals) at 1:100 dilution and Alexa Fluor 594 secondary antibody (Cambridge BioScience). Images were

Table 1

Genomic Primers for PCR Amplification of *KIND1*

Primer	Sequence	Position Before/After Exon	Annealing Temperature (°C)	Product Size (bp)
KIND1F	AAATCTGCAGACTGCGCCTC	−372[a]	60	473
KIND1R	GAGGCTGCAGAAAGAAAGGG	+101		
KIND2F	ATATCTGGAGCACCTGGAAC	−150	58	401
KIND2R	ATTGCTCTCCAGGGCATTAC	+116		
KIND3F	TGAGGAGCTGGAGATCAGTT	−123	58	416
KIND3R	GAAGTAGGCAGAATGCACAC	+83		
KIND4F	GACCCTGAGTCTTAGAAGGA	−67	58	343
KIND4R	GCCTTTCCTCATCACATCAG	+129		
KIND5F	CAGTGCCCAGCTTGACTTAT	−144	58	455
KIND5R	ATCCCTAGGCCTACCAACTT	+97		
KIND6F	CAGTGCTCAGAAAGTGTCAG	−186	58	407
KIND6R	GCTAAACAGGCGATCACACA	+118		
KIND7F	CTGAGCTGAAGTTTGCTGCA	−117	58	434
KIND7R	GTGTGTGGATTATGAGGAGC	+209		
KIND8F	AAGGAGACCTCTGTTTAGGA	−133	56	404
KIND8R	CTTGTTAGGTGAAGAGCATC	+139		
KIND9F	GTAGCGAGTGTAAACTGAAG	−168	56	315
KIND9R	ACCTTTGAACCATGAACCTG	+109		
KIND10F	TGCAGCGTGTTCCACATTTC	−60	58	257
KIND10R	GGATTACAGGTTTGAGCCAC	+72		
KIND11F	ACAGATGCCTCAGAACTCAG	−46	58	208
KIND11R	TGCTCTTAGGCTTAGTGGAG	+55		
KIND12F	GCTTTGCACTTGAGCTTGCT	−43	58	375
KIND12R	GTGCTGGAATTACAGGTGTG	+110		
KIND13F	CTAACAGGGTGATCACAGAG	−66	56	269
KIND13R	CTAAATGAGAAAACTGGGGCT	+78		
KIND14F	CTTCATTGTCCATTCCTCTG	−123	58	328
KIND14R	CAATTCTGAGGGACACACAT	+60		
KIND15F	CCAGTCCAGCAAAGCACTTT	−74	58	343
KIND15R	GTCCAGAATCTACATGCTGG	+95[b]		

[a] Before end of exon.
[b] After TGA.

taken on a Zeiss LSM510 META laser-scanning confocal microscope, using an α-Plan Fluar × 100 objective and an optical section of 0.7 μm.

Results

Patients with Kindler Syndrome from Bocas del Toro, Panama

Patients in the Panamanian cohort that we studied have clinical findings quite similar to those of the patient whom Kindler (1954) originally studied. These include congenital acral blisters, blistering after trauma or sun exposure, erythema and itching after sun exposure, and patchy hyper- and hypopigmentation with atrophy and telangiectases (poikiloderma) developing in early childhood in both sun-exposed and nonexposed skin. Other features include hyperkeratosis of the palms and soles and diffuse cutaneous atrophy and wrinkling, particularly on the dorsa of the hands and feet (fig. 1). Other mucocutaneous features include periodontal disease, dental caries, and phimosis. Typically, the blistering and photosensitivity improve markedly in adulthood, but the poikiloderma persists. Some variability in phenotypic severity existed, particularly in the degree of photosensitivity, the age at onset of poikiloderma, and the degree of hyperkeratosis. All patients examined were <40 years of age.

Linkage of Kindler Syndrome to 20p12.3

After excluding linkage to the *RecQ1* and *RecQ5* genes, candidates selected because of the phenotypic similarity of Kindler syndrome to Rothmund-Thomson syndrome and Bloom syndrome (MIM 210900), we performed a genomewide scan on DNA from 24 individuals from the Panamanian cohort—16 with Kindler syndrome and 8 unaffected family members. A cluster of markers (D20S846, D20S115, and D20S851) on 20p12.3 cosegregated with the disease, giving a maximum two-point LOD score of 2.48 at recombi-

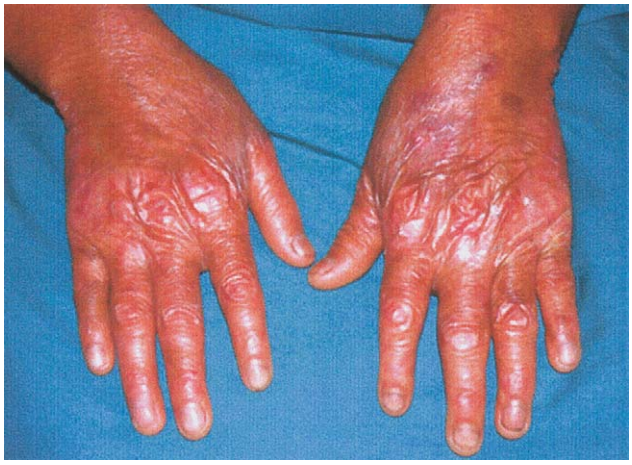

Figure 1 Clinical features. Atrophy, wrinkling, and abnormal pigmentation are shown on the hands of a Panamanian young adult with Kindler syndrome.

nation fraction (θ) 0 with D20S846. False linkage was detected initially with D20S107 on 20q12 ($Z_{max} = 2.59$ at $\theta = 0$) but subsequently was excluded by analysis of additional Panamanian families. We then genotyped further Panamanian individuals over a 3.6-Mb area surrounding D20S846. Observed recombinants and the shared haplotype narrowed the critical interval to a 0.6-cM area of homozygosity between D20S95 and D20S192 (Généthon genetic map), corresponding to 280 kb of genomic DNA (fig. 2). Patients with Kindler syndrome from consanguineous families from Italy, Oman, Jordan, Turkey, Afghanistan, and Saudi Arabia showed homozygosity across the same region, leading to a maximum multipoint LOD score of 11.7 at $\theta = 0$ with D20S905.

Identification of the Kindler Syndrome Gene, KIND1

Six experimentally verified and/or strongly predicted genes were identified within the critical interval between D20S95 and D20S192, by study of the Human Genome Browser (UCSC Genome Bioinformatics). These were *CHGB, LOC51605, MGC4816, LOC54675, FLJ20116,* and *BMP2*. We sequenced the predicted exons for all these genes and identified mutations in only one of the six: *FLJ20116,* subsequently renamed "*KIND1*" (encoding the protein kindlin-1). The UCSC annotation for *FLJ20116* predicted a gene of seven exons that encodes a predicted protein of 230 amino acids; however, RT-PCR of keratinocyte mRNA identified a 4,931-bp transcript encoded by a 15-exon gene, with the initiating methionine in exon 2 and a stop codon in exon 15. Northern blotting confirmed the latter, 4.9-kb mRNA as the major transcript (see the "Tissue Expression of *KIND1*" subsection, below; also see fig. 3). The gene spans 48.5 kb of genomic DNA, and exon sizes range from 47 to 234 bp. The predicted ORF is 2,034 bp, encoding a protein of 677 amino acids with a calculated molecular weight of 77.3 kDa. The predicted exon sizes and acceptor/donor splice sites (table 2) all were confirmed by RT-PCR.

Kindlin-1 Protein Structure

Analysis of the primary protein structure of the kindlin-1 polypeptide revealed a number of features predicting that the function of this molecule relates to anchorage of the actin cytoskeleton to the plasma membrane:

First, BLAST analysis (NCBI) revealed that kindlin-1 has C-terminal homology to talin and N-terminal homology to the *Dictyostelium* talin homolog, filopodin (fig. 4*A*). Both of these proteins are involved in anchorage of the actin cytoskeleton in focal contacts (Critchley 2000), which are membrane-substrate attachment structures observable in cultured cells (Zamir and Geiger 2001*a,* 2001*b*).

Second, Conserved Domain BLAST analysis showed that kindlin-1 possesses a centrally located pleckstrin homology (PH) domain (fig. 4*A*). PH domains mediate associations with specific phosphatidylinositol phospholipid species in the plasma membrane and are a feature of a number of cytoskeletal-associated and/or cell-signaling molecules (Maffucci and Falasca 2001; Itoh and Takenawa 2002; Lemmon et al. 2002).

Third, kindlin-1 also possesses two regions of homology with the FERM (filopodin and ezrin/radixin/moesin) domain, which is shared by erythrocyte protein 4.1, ERM (ezrin, radixin, and moesin) proteins, and a number of proteins that again mediate anchorage of the cytoskeleton to the plasma membrane (Chishti et al. 1998). In kindlin-1, the first FERM-domain homology region aligns to residues 49–133 of the 207-amino-acid FERM-domain consensus sequence (NCBI Conserved Domain Database); the second region aligns to residues 126–207 of the consensus sequence. Thus, kindlin-1 possesses an unusual, bipartite FERM domain that is interrupted by a PH domain. Both of these structural features imply that kindlin-1 is involved in membrane and/or cytoskeleton association.

A Family of Kindlin-Related Proteins

Kindlin-1 shows closest homology (30% amino acid identity) to the *Caenorhabditis elegans* protein UNC-112 (fig. 4*B*). By a translated BLAST search of the human genome sequence, we identified two further proteins with significant overall homology to UNC-112. These were MIG-2 (with 42% amino acid identity) and the predicted protein MGC10966 (with 38% amino acid identity) (fig. 4*B*). The three human proteins and UNC-112 are very similar in size and share the same protein-

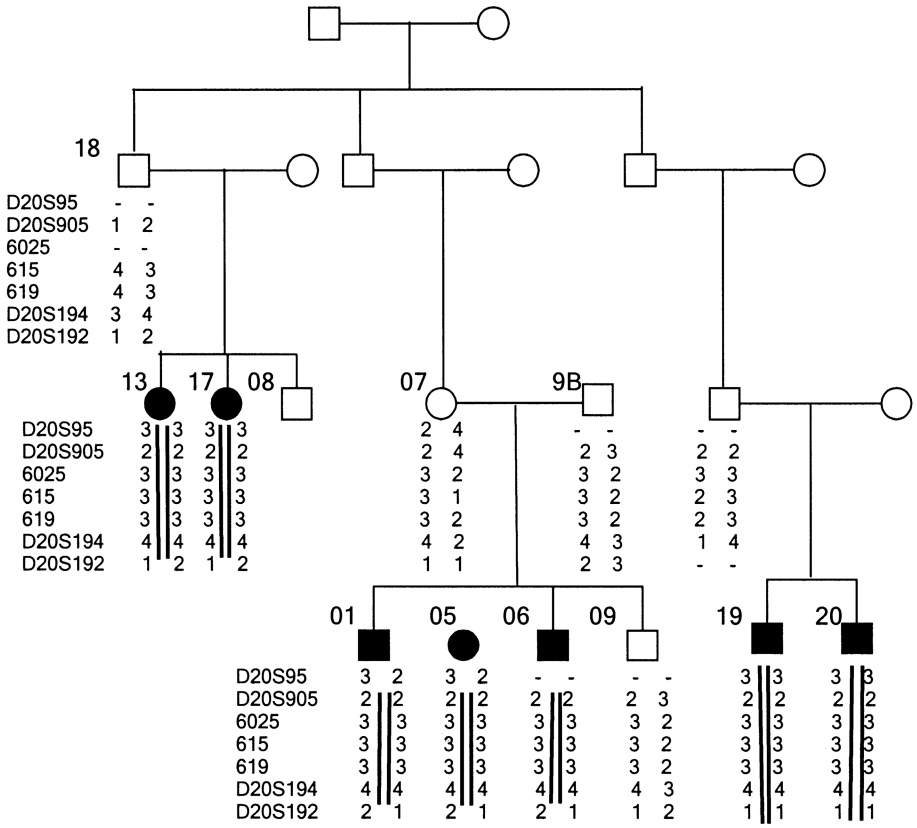

Figure 2 Haplotype analysis of a Panamanian family with Kindler syndrome. Genotype data are shown below the symbol for each affected individual. Haplotypes that delineate the Kindler syndrome critical interval are indicated by black bars. Markers 6025, 615, and 619 were derived from analysis of the sequence of the Human Genome Browser (UCSC Genome Bioinformatics).

domain organization and talin/filopodin homology regions (fig. 4*A*). This domain organization appears to be unique to the kindlin family of proteins (NCBI Conserved Domain Database and Pfam). Evolutionary analysis by the unweighted pair group method with arithmetic mean (UPGMA) (Nei 1987, pp. 293–298) revealed that kindlin-1 and MIG-2 are more closely related and more recently diverged from MGC10966 (fig. 4*C*). Overall, MIG-2 shows the closest amino acid similarity to UNC-112.

MIG-2 (mitogen-induced gene 2 [GenBank accession number Z24725]) has 62% amino acid identity with kindlin-1 and is located on 14q22.1. (Note that a *C. elegans* gene named "*mig-2*" [Zipkin et al. 1997] is neither structurally nor functionally related to the human *MIG-2* gene [Wick et al. 1994]; therefore, to avoid confusion, we suggest that human *MIG-2* be renamed "kindlin-2" [gene name "*KIND2*"] because of its close homology to kindlin-1.) *MIG-2* was originally isolated by differential cDNA library screening as a serum-inducible gene expressed in human fibroblasts (Wick et al. 1994). The gene was thought to be encoded partly by an antisense transcript of the transcription factor gene *TCF12* (also known as "*HTF4*") (Wick et al. 1994); however, in agreement with published mapping data (Zhang et al. 1995), the near-complete human genome data localize *TCF12* to 15q21.3, not 14q22.1. We found that the antisense strand of the 3′ UTR of *MIG-2* indeed possesses regions of similarity to the *TCF12* transcript; however, the most homologous area is only 42% identical. Furthermore, this homology is shared by the 3′ UTRs of the *KIND1* and *KIND3* transcripts. The functional significance, if any, of this antisense homology remains to be elucidated.

The other human homolog of *KIND1* is the predicted gene *MGC10966* (GenBank accession number NM_031471), located in a gene-dense region on 11q13.1. We propose that this gene, encoding the protein kindlin-3, be renamed "*KIND3*." The predicted polypeptide is 49% identical to kindlin-1 and 53% identical to kindlin-2. Interestingly, this transcript has an additional region of antisense homology within its 3′ UTR. Part of the 3′ UTR is shared with the 3′ UTR of a gene located upstream and expressed from the opposite strand—the human ortholog of *Tpt1h*, the murine tRNA splicing 2′ phosphotransferase gene. The entire *KIND3* and *TPT1H* genes exist within

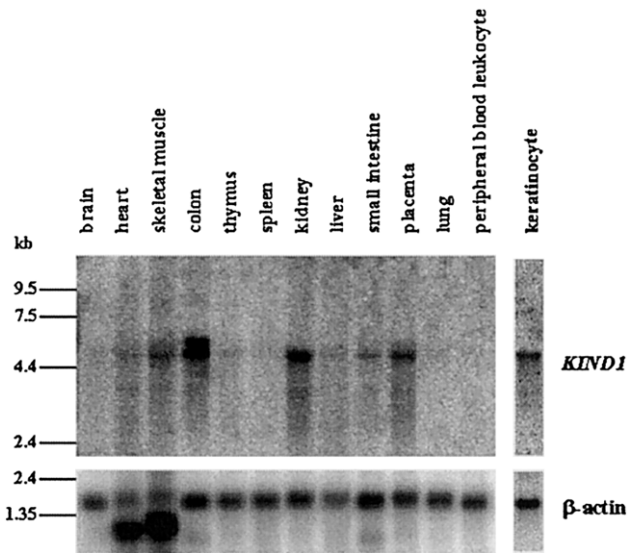

Figure 3 Multiple-tissue and keratinocyte northern blots hybridized with *KIND1* and *β*-actin probes. Expression of a 4.9-kb *KIND1* transcript is present predominantly in keratinocyte, colon, kidney, and placenta and at lower levels in heart, skeletal muscle, liver, and small intestine. An additional transcript, of ~5.8-kb, is present in colon.

intronic sequences of the *LRP16* gene (see the UCSC Genome Bioinformatics Web site).

Tissue Expression of KIND1

Hybridization of a *KIND1* cDNA probe to a multiple-tissue northern blot showed tissue-specific expression. The *KIND1* transcript is predicted to be 4.9 kb, and a transcript of this size was detected in cultured epidermal keratinocytes, colon, kidney, and placenta and at lower expression levels in heart, skeletal muscle, liver, and small intestine (fig. 3). Colon contains an additional transcript that is ~5.8 kb. The June 2002 UCSC Human Genome Working Draft includes an intragenic EST found in colon (*FLJ21712* [clone COL10231] [GenBank accession number AK025365]), which could represent a further translated exon between exons 8 and 9. Furthermore, the November 2002 UCSC Human Genome Working Draft also provides evidence for alternative exons 11 and 15.

Differential Expression of Human Kindlin Genes

Multiple-tissue cDNA panels showed significant differences in expression of the three kindlin genes (table 3). In particular, *KIND1* is highly expressed in keratinocytes, with lower expression in prostate, ovary, colon, kidney, and pancreas and weak expression in spleen, thymus, testis, heart, brain, placenta, lung, liver, and fibroblasts. The high expression in cultured keratinocytes and the low expression in cultured fibroblasts were confirmed by quantitative PCR (data not shown). No expression is seen in small intestine, peripheral blood leukocytes, or skeletal muscle. *KIND2* shows only moderate expression in spleen, prostate, testis, ovary, small intestine, colon, heart, placenta, lung, liver, kidney, pancreas, and fibroblasts and weak expression in thymus, brain, skeletal muscle, and keratinocytes. In contrast, *KIND3* shows high expression in spleen, thymus, and peripheral blood leukocytes and moderate-to-low expression in prostate, testis, ovary, small intestine, colon, heart, brain, placenta, lung, liver, skeletal muscle, kidney, and pancreas. No expression of *KIND3* was observed in cultured keratinocytes or fibroblasts.

Detection of Loss-of-Function Mutations in KIND1

By direct nucleotide sequencing, we identified homozygous nonsense or frameshift mutations in 17 families with Kindler syndrome (table 4). All 26 patients from Bocas del Toro shared the same homozygous nonsense mutation, R271X (fig. 5*D*). This mutation also was identified in patients from three additional families (two white families from the United States and one Middle Eastern Omani family). Haplotype analysis of common *KIND1* polymorphisms in these families indicated that the mutation likely arose on different genetic backgrounds in geographically diverse families (data not shown). A second recurrent nonsense mutation, R288X (fig. 5*E*), was identified in British and Turkish families, again embedded within different haplotypes. Details of the other pathogenic mutations are shown in table 4 and figures 5*A*–5*F*. All sequence variants were excluded in 100 ethnically matched control chromosomes by direct sequencing or restriction-endonuclease digestion.

In five additional inbred families, homozygosity by descent was observed at the *KIND1* locus; however, we were unable to detect mutations by our genomic PCR strategy. It is possible that these families carry promoter defects or other cryptic mutations. Two additional families (one from Canada [Haber and Hanna 1996] and the other from the United States, with one parent of European descent and the other of African descent) did not show linkage to the *KIND1* locus; however, both of these families showed clinical differences from the Panamanian kindred (Haber and Hanna 1996). Thus, there may be a disorder that is clinically similar to but genetically different from Kindler syndrome.

Localization of Kindlin-1 in Skin

An affinity-purified polyclonal antibody was produced against a C-terminal synthetic peptide of kindlin-1. This stained normal control skin throughout the epidermis and, in particular, gave strong, cytoplasmic labeling of basal keratinocytes with a linear pattern at the dermal-epidermal junction (fig. 6*A*). In contrast, there was markedly reduced staining in skin from patients with Kindler

Table 2

Genomic Organization of *KIND1*

Exon	3′ Acceptor Sequence[a]	Exon Size (bp)	5′ Donor Sequence[a]	Intron Size (bp)
1	…	771	AAGGAG***gt***gggtgctc	3,201
2	tgttcagc***ag***ACACCA	169	AGATCA***gt***aagttact	3,359
3	atttttgc***ag***ATATAT	234	TCCTGA***gt***aagtaccc	3,187
4	ttatttct***ag***ATATTA	147	CATCAG***gt***aagacttg	1,965
5	tgccttgc***ag***TAAGTC	214	TGCAGG***gt***aaggacac	2,663
6	cattttct***ag***TTGGCT	103	CCTAAA***gt***aagcaact	9,900
7	ttgtctct***ag***TATGAT	108	CTACAG***gt***atgggaac	490
8	ttcattttt***ag***TACCAC	132	CTTTTG***gt***atgaactt	1,913
9	tttttctt***ag***GAGGAC	50	ATTTAG***gt***aagtaaac	5,899
10	gaatttgc***ag***GCCCAA	125	TTAGAG***gt***aagagtac	1,081
11	tgtccttc***ag***GCTGCG	107	GACCAT***gt***gagtaaaa	2,489
12	tttgctgc***ag***GAGAAT	222	AAACAG***gt***actgttaa	901
13	ttctgttc***ag***CTGGCC	125	TGTCAG***gt***gattacaa	4,462
14	ttcttttc***ag***ATTTAA	142	CGGCAG***gt***aaagtgaa	2,089
15	cctcttcc***ag***GTGGTC	2,282[b]	…	

[a] Lowercase letters represent the intronic sequence, and uppercase letters represent the exonic sequence. The intronic acceptor/donor splice sites are shown in boldface italic.

[b] Up to and including polyadenylation signal AATAAA.

syndrome (fig. 6*B*), and, specifically, staining of basal keratinocytes was virtually absent. There was no visible staining in either control or patient skin in the dermis. Thus, the kindlin-1 protein, as recognized by this antibody, appears to be localized solely within the epidermis and particularly in basal keratinocytes.

Localization of Kindlin-1 in Epithelial Cells

We transiently expressed full-length EGFP-kindlin-1 (i.e., EGFP fused to the N-terminus of kindlin-1) in epithelial cell line PtK2 and examined the resultant expression pattern by confocal laser-scanning microscopy. Cells expressing high levels of the fusion protein gave only diffuse staining patterns (data not shown). In some cells that transiently expressed moderate levels of EGFP-kindlin-1, we observed filamentous staining that colocalized with filamentous actin labeled with fluorescent phalloidin (fig. 7*A*). These actin filament bundles were seen to terminate in putative attachment structures reminiscent of focal contacts. In cells that expressed EGFP-kindlin-1 at very low levels, in which the EGFP background haze was much lower, these attachment structures could be seen more clearly, and EGFP-kindlin-1 colocalized with vinculin, a marker for focal contacts (fig. 7*B*). Localization to focal contacts was very reproducible but was not observed in all EGFP-expressing cells. These data indicate that kindlin-1 is likely a hitherto-unrecognized component of focal contacts directly or indirectly associated with filamentous actin within focal contacts. Identical colocalization data were obtained when EGFP-kindlin-1 was expressed in normal human primary keratinocytes (data not shown); however, because of their flat morphology, colocalization was seen more readily in PtK2 cells.

Discussion

We have showed that loss of epidermal kindlin-1 expression is the molecular basis of Kindler syndrome, an autosomal recessive genodermatosis characterized by skin fragility, poikiloderma, photosensitivity, and premature skin aging. Kindlin-1 is a protein of predicted molecular mass 77.3 kDa that contains regions of homology to talin and filopodin and has both a bipartite FERM domain and a PH domain, all of which are indicative of association with plasma-membrane adhesion structures and the actin cytoskeleton (Maffucci and Falasca 2001; Itoh and Takenawa 2002; Lemmon et al. 2002) (fig. 4*A*). Here, we have experimentally showed that kindlin-1 colocalizes with vinculin and therefore is a component of focal contacts (fig. 7*B*), which are structures involved in membrane-substratum attachment in cultured cells, and also can associate, to some extent, with filamentous actin (fig. 7*A*). We have identified two additional kindlinlike proteins from the human genome: kindlin-2 (MIG-2) and kindlin-3 (MGC10966). All three kindlins are closely related, in amino acid sequence and protein-domain organization, to the *C. elegans* focal-contact protein UNC-112 (Rogalski et al. 2000). This protein-domain configuration appears to be unique to the kindlin family.

In nematodes, loss-of-function mutations in UNC-112 give rise to the *pat* (paralyzed, arrested elongation at twofold) phenotype (Rogalski et al. 2000). This phenotype can result from mutations in molecules that

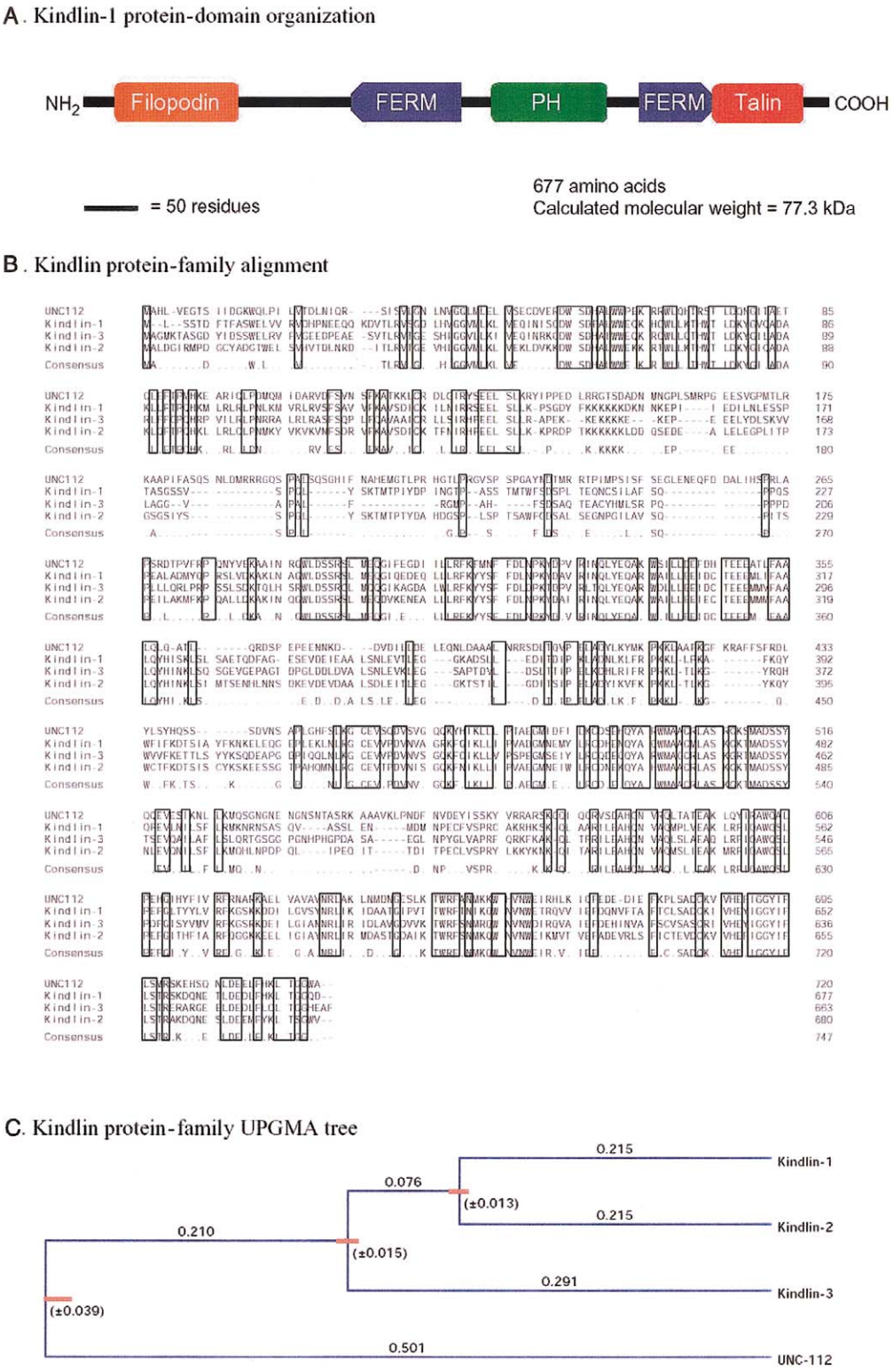

Figure 4 Kindlin-1 protein-domain organization. *A*, Schematic representation of the FERM, PH, and talin homology domains of kindlin. *B*, Amino acid sequence alignment between members of the human kindlin family and their *C. elegans* ortholog UNC-112. The overall amino acid sequence identity is high (41%) between the two species. *C*, Evolutionary tree analysis by UPGMA, showing that kindlin-1 and kindlin-2 are more related and more recently diverged from kindlin-3. Protein alignments and UPGMA analysis were performed by use of the Geneworks 2.5 analysis package (Oxford Molecular Group).

Table 3

RT-PCR Tissue-Expression Profiles of the KIND-Family Genes

	Expression[a] of		
	KIND1	*KIND2*	*KIND3*
Spleen	+	++	+++
Thymus	+	+	+++
Prostate	++	++	+
Testis	+	++	+
Ovary	++	++	++
Small intestine	−	++	++
Colon	++	++	++
Leukocyte	−	−	+++
Heart	+	++	+
Brain	+	+	+
Placenta	+	++	++
Lung	+	++	++
Liver	+	++	++
Skeletal muscle	−	+	+
Kidney	++	++	+
Pancreas	++	++	++
Keratinocyte	+++	+	−
Fibroblast	+	++	−
Control cDNA	++	++	++

[a] − = No expression; + = weak expression; ++ = moderate expression; +++ = strong expression.

anchor the actin-myosin cytoskeleton in the muscle via transmembrane complexes (especially α- and β-integrins) to the ECM—in particular, to the major heparin sulfate proteoglycan, perlecan. UNC-112 binds to a molecule with potential adapter and signaling functions—namely PAT-4, the worm homolog of integrin-linked kinase (ILK) (Mackinnon et al. 2002). During assembly of junctions of muscle cells to the ECM, PAT-4/ILK and UNC-112 function after integrins have marked the sites of the nascent junctions and before deposition of vinculin and attachment of actin filaments (Rogalski et al. 2000; Mackinnon et al. 2002). ILK has been shown to function primarily as a structural molecule by direct binding to the first 32 N-terminal residues of UNC-112, and kinase-deficient forms of ILK can rescue the *pat-4* phenotype in worms (Mackinnon et al. 2002). However, the N-termini of all three human kindlin proteins lack homology to the ILK binding site of UNC-112 (fig. 4*B*). Therefore, this function may have been modified or lost in mammalian homologs. Ultrastructurally, in Kindler syndrome, there is marked disorganization of skin basement membrane, with reduplication of lamina densa and cleavage at or close to the dermal-epidermal junction (Shimizu et al. 1997). We too have found extensive basement-membrane reduplication, in several of the patients described here. Significantly, therefore, the loss of cytoskeletal-ECM adhesion noted in nematodes carrying mutations in UNC-112 would seem to be analogous to the adhesive defect observed in the skin of patients with Kindler syndrome. These morphological features underscore the significance of kindlin-1 in the construction/regulation of a normally functioning epidermal basement membrane.

The many forms of epidermolysis bullosa and related skin fragility diseases can be considered as analogous to the muscular dystrophies. Thus, genetic diseases of both organ systems can be caused by defects in any one component of a chain of molecules that connect the cytoskeleton to the ECM. In human inherited muscle diseases, the underlying genetic defects more commonly occur in a series of molecules that connect the actin-myosin cytoskeleton via actin-binding proteins (dystrophin) through a transmembrane complex (dystroglycans) to the basement membrane (laminin 2) and, subsequently, to the ECM (collagens such as collagen VI). Alternatively, defects in the muscle intermediate-filament protein desmin can cause myopathy (Munoz-Marmol et al. 1998). Similarly, in the skin, a series of proteins connect the basal-keratinocyte intermediate-filament cytoskeleton (keratins K5 and K14) through the hemidesmosome trans-

Table 4

Mutations Identified in Individuals with Kindler Syndrome

Geographic Origin (No. of Patients)	Nucleotide Change	Predicted Consequence[a]	Exon
Jordan (2)	C193T	Q65X	3
Italy (1)	373delT	I124fs	3
Pakistan (1)	G614A	W205X	5
Panama (26)	C811T	R271X	6
United States (2)	C811T	R271X	6
Oman (2)	C811T	R271X	6
Britain (1)	C862T	R288X	7
Turkey (1)	C862T	R288X	7
Japan (2)	1089delG or IVS8+1delG (splice donor)	L363fs or IVS8+1delG (splice donor)	8

Note.—Nucleotide positions correspond to the *KIND1* coding sequence as deposited in GenBank (accession number AY137240, submitted July 2002). del = Deletion; fs = frameshift.

[a] Either a frameshift or a splice-donor mutation.

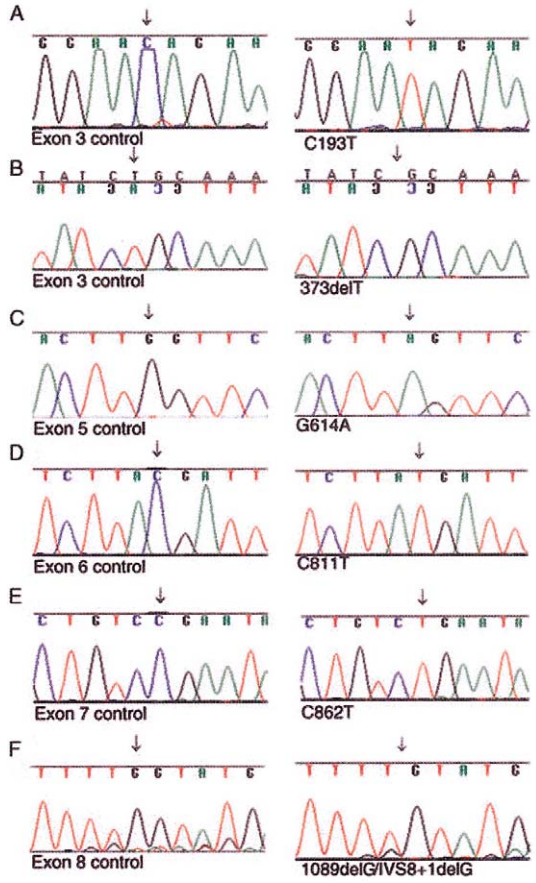

Figure 5 Nucleotide sequencing of DNA from patients with Kindler syndrome and unaffected control individuals, demonstrating pathogenic homozygous nonsense or frameshift mutations. *A,* Nucleotide transition 193C→T, predicting amino acid change Q65X, in two Jordanian siblings. *B,* Deletion mutation 373delT in an Italian patient. *C,* 614G→A, predicting W205X, in a Pakistani patient. *D,* 811C→T, predicting amino acid change R271X, in the Panamanian families, the Omani sibship, and two unrelated Americans. *E,* Transition mutation 862C→T, predicting R288X, in a British patient and a Turkish patient. *F,* Deletion mutation in two unrelated Japanese patients, representing either 1089delG or IVS8+1delG.

membrane complex (plectin, BPAG1, $\alpha 6\beta 4$ integrin, and collagen XVII) to the basement membrane (laminin 5) and, subsequently, to the ECM (collagen VII). Interestingly, loss of plectin causes both muscle disease and skin blistering (McLean et al. 1996), a phenotype explicable by plectin's participation in linking keratins to the inner plaque of hemidesmosomes in skin (Smith et al. 1996) and also in linking desmin within the Z-lines of striated muscle (Reipert et al. 1999). Kindler syndrome appears to complete the tetrad of actin-ECM and intermediate-filament–ECM linkage diseases of skin and muscle. The apparent lack of muscle disease in patients with Kindler syndrome suggests that the function performed by UNC-112 in *C. elegans* muscle presumably has been replaced in mammals by the dystrophin-dystroglycan system, in which a more specialized and robust linkage system may be needed to withstand the more demanding structural requirements of vertebrate muscle. Since kindlin-1 is very strongly expressed in keratinocytes but is absent from skeletal muscle (table 3) and since the other two kindlins are more widely expressed, it is possible that the latter make a more important contribution to actin-ECM linkage in muscle and other tissues. In particular, kindlin-3 is very strongly expressed in leukocytes, spleen, and thymus, so the main function of this protein may be immune system related (table 3).

More than 50 proteins have been shown to associate with focal contacts, where they perform structural and/or signaling functions (Zamir and Geiger 2001*a*, 2001*b*). It remains to be seen whether the main function of kindlin-1 is primarily that of structural tethering or whether it is that of regulation and/or recruit-

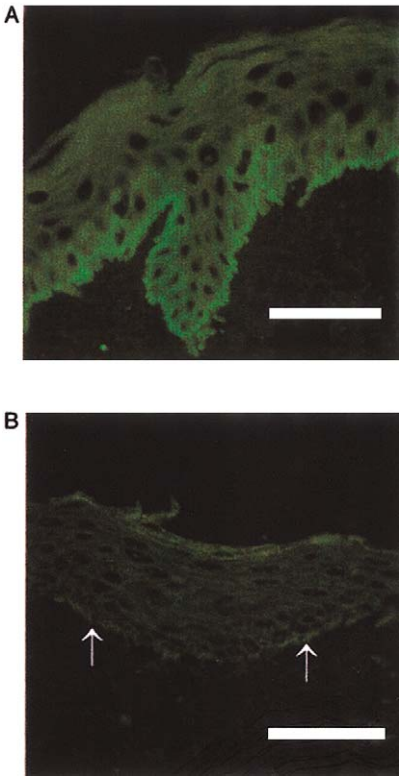

Figure 6 Immunohistochemical changes in Kindler syndrome epidermis. *A,* Immunofluorescence labeling with affinity-purified anti-kindlin-1 polyclonal antibody in normal control skin reveals bright intracellular and cell-surface labeling within the epidermis, especially in the basal-keratinocyte layer. Linear labeling is seen at the dermal-epidermal junction. *B,* Skin from a patient with Kindler syndrome, showing almost-complete absence of immunostaining. The dermal-epidermal junction is indicated with arrows. Scale bar = 50 μm.

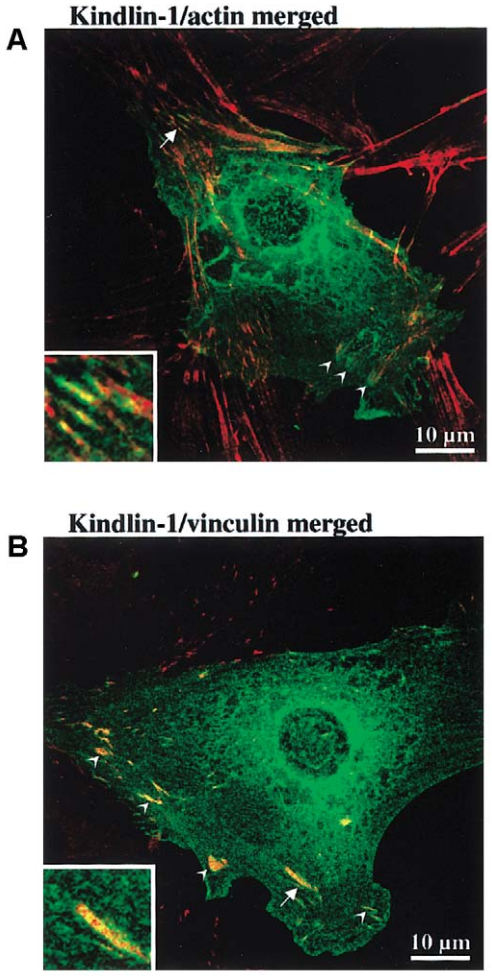

Figure 7 Intracellular localization of kindlin-1 in epithelial cell line PtK2. *A,* Merged confocal laser-scanning micrograph of PtK2 cells, transiently transfected with EGFP-kindlin-1 (*green*) and stained with Alexa Fluor 594 phalloidin to reveal filamentous actin (*red*). The ends of actin stress fiber bundles exhibit coalignment with EGFP-kindlin-1 to produce the orange coloration in this merged image (*arrowheads*). These structures were reminiscent of focal contacts. The area marked by the arrow is enlarged in the inset, where the colocalization can be seen more easily. *B,* Merged confocal laser-scanning micrograph of PtK2 cells transiently transfected with EGFP-kindlin (*green*) and stained for vinculin by indirect immunofluorescence using Alexa Fluor 594 (*red*) to reveal focal contacts. Focal contacts (*arrowheads*) are seen to coalign with EGFP-kindlin to produce the orange coloration in this merged image. Some faint colocalization with cytoskeletal structures also can be seen. The area marked by the arrow is enlarged in the inset, where the colocalization can be seen more easily. These data confirmed that kindlin-1 is a component of focal contacts.

ment of other molecules mediating actin-ECM adhesion. Here, we have observed that not all cells expressing EGFP-kindlin-1 localize this protein to focal contacts. One possible explanation is that kindlin-1 may have to associate with another factor(s) to enter focal contacts. In cells expressing very high levels of EGFP-kindlin-1, the cytoplasmic pool of this recruitment factor may become exhausted, preventing most of the putatively overexpressed EGP-kindlin-1 from associating with focal contacts. In view of this observation and the immensely complex molecular architecture of focal contacts (Zamir and Geiger 2001*a*, 2001*b*), the identification of protein and phospholipid binding partners of kindlin-1 and its relatives by yeast two-hybrid analysis, coimmunoprecipitation, and blot overlays is a logical next step in elucidating the function of this protein family.

In view of the skin blistering observed in younger patients with Kindler syndrome, it is tempting to speculate that kindlin-1 is a structural molecule, although this mechanical defect also could be secondary to a signaling or organizational/recruitment role. The extensive reduplication of basement membrane seen in the skin of these patients suggests that loss of kindlin-1 from membrane-bound attachment structures at the dermal-epidermal junction induces basal keratinocytes to oversecrete basement-membrane components. Since many proteins containing PH domains are involved in signal transduction (Maffucci and Falasca 2001), kindlin-1 could play a regulatory role in the inhibition of basement-membrane synthesis.

One unexplained clinical phenomenon is the waning of blistering in older children, although such changes are well recognized in other inherited skin fragility disorders, especially autosomal dominant cases of epidermolysis bullosa simplex resulting from mutations in keratin 14 or keratin 5 (Smith 2003). However, spontaneous improvement is rare in autosomal recessive blistering skin disorders. Mechanistically, in Kindler syndrome, it is possible that the reliance of newborn epidermis on the actin-ECM and intermediate-filament–ECM associations is more balanced but that, by adulthood, the contribution of the former lessens. Genotype-phenotype correlations are difficult to assess, because of the variability of clinical severity both between patients at different ages and among patients within the same family with the same mutation. More puzzling is the nature of the link between loss of kindlin-1 protein and the pathogenesis of other clinical findings—in particular, the photosensitivity and skin atrophy, resembling findings in helicase-deficient diseases, such as Rothmund-Thomson syndrome and Bloom syndrome. Future functional studies will help elucidate the mechanisms causing these interesting phenotypic abnormalities.

Acknowledgments

We are grateful to the patients for their participation in this study. The work was supported by an Individual Na-

tional Research Service Award from the National Institute of Arthritis and Musculoskeletal and Skin Diseases (AR 123456) and a fellowship from the Society for Pediatric Dermatology (to D.H.S.), Action Research, the Dystrophic Epidermolysis Bullosa Research Association (UK) and the British Skin Foundation. W.H.I.M. and F.J.D.S. are funded by a Wellcome Trust Senior Research Fellowship (to W.H.I.M.). The Centre for High-Resolution Imaging and Processing, Dundee, is supported by the Medical Research Council and the Wellcome Trust. We thank Galderma, for the generous donation of sunscreen for patients in Panama, and Christina Walker and Fintan Coleman, for their help in preparation of the manuscript.

Electronic-Database Information

Accession numbers and URLs for data presented herein are as follows:

GenBank, http://www.ncbi.nlm.nih.gov/Genbank/ (for *KIND1* [accession number AY137240], *MIG-2* [accession number Z24725], *MGC10966* [accession number NM_031471], and *FLJ21712* [clone COL10231] [accession number AK025365])

NCBI Conserved Domain Database, http://www.ncbi.nlm.nih.gov/Structure/cdd/cdd/shtml

Online Mendelian Inheritance in Man (OMIM), http://www.ncbi.nlm.nih.gov/Omim/ (for Kindler syndrome, dystrophic epidermolysis bullosa, Rothmund-Thomson syndrome, and Bloom syndrome)

Pfam, http://www.sanger.ac.uk/Software/Pfam/search.shtml

UCSC Genome Bioinformatics, http://genome.ucsc.edu/ (for Human Genome Browser)

References

Al Aboud K, Al Hawsawi K, Al Aboud D, Al Githami A (2002) Kindler syndrome in a Saudi kindred. Clin Exp Dermatol 27:673–676

Bleck O, Abeck D, Ring J, Hoppe U, Vietzke JP, Wolber R, Brandt O, Schreiner V (1999) Two ceramide subfractions detectable in Cer(AS) position by HPTLC in skin surface lipids of non-lesional skin of atopic eczema. J Invest Dermatol 113:894–900

Chishti AH, Kim AC, Marfatia SM, Lutchman M, Hanspal M, Jindal H, Liu SC, et al (1998) The FERM domain: a unique module involved in the linkage of cytoplasmic proteins to the membrane. Trends Biochem Sci 23:281–282

Church DM, Stotler CJ, Rutter JL, Murrell JR, Trofatter JA, Buckler AJ (1994) Isolation of genes from complex sources of mammalian genomic DNA using exon amplification. Nat Genet 6:98–105

Critchley DR (2000) Focal adhesions—the cytoskeletal connection. Curr Opin Cell Biol 12:133–139

Ganguly A, Rock MJ, Prockop DJ (1993) Conformation-sensitive gel electrophoresis for rapid detection of single-base differences in double-stranded PCR products and DNA fragments: evidence for solvent-induced bends in DNA heteroduplexes. Proc Natl Acad Sci USA 90:10325–103329

Haber RM, Hanna WM (1996) Kindler syndrome: clinical and ultrastructural findings. Arch Dermatol 132:1487–1490

Itoh T, Takenawa T (2002) Phosphoinositide-binding domains: functional units for temporal and spatial regulation of intracellular signalling. Cell Signal 14:733–743

Kindler T (1954) Congenital poikiloderma with traumatic bulla formation and progressive cutaneous atrophy. Br J Dermatol 66:104–111

Lemmon MA, Ferguson KM, Abrams CS (2002) Pleckstrin homology domains and the cytoskeleton. FEBS Lett 513:71–76

Mackinnon AC, Qadota H, Norman KR, Moerman DG, Williams BD (2002) *C. elegans* PAT-4/ILK functions as an adaptor protein within integrin adhesion complexes. Curr Biol 12:787–797

Maffucci T, Falasca M (2001) Specificity in pleckstrin homology (PH) domain membrane targeting: a role for a phosphoinositide-protein co-operative mechanism. FEBS Lett 506:173–179

McLean WHI, Pulkkinen L, Smith FJD, Rugg EL, Lane EB, Bullrich F, Burgeson RE, Amano S, Hudson DL, Owaribe K, McGrath JA, McMillan JR, Eady RAJ, Leigh IM, Christiano AM, Uitto J (1996) Loss of plectin causes epidermolysis bullosa with muscular dystrophy: cDNA cloning and genomic organization. Genes Dev 10:1724–1735

Munoz-Marmol AM, Strasser G, Isamat M, Coulombe PA, Yang Y, Roca X, Vela E, Mate JL, Coll J, Fernandez-Figueras MT, Navas-Palacios JJ, Ariza A, Fuchs E (1998) A dysfunctional desmin mutation in a patient with severe generalized myopathy. Proc Natl Acad Sci USA 95:11312–11317

Navsaria H, Sexton C, Bouvard V, Leigh I (1994) Growth of keratinocytes with a 3T3 feeder layer: basic techniques. In: Leigh I, Watt F (eds) Keratinocyte methods. Cambridge University Press, Cambridge, UK, pp 5–12

Nei M (1987) Molecular evolutionary genetics. Columbia University Press, New York

O'Connell JR, Weeks DE (1995) The VITESSE algorithm for rapid exact multilocus linkage analysis via genotype set-recoding and fuzzy inheritance. Nat Genet 11:402–408

——— (1998) PedCheck: a program for identification of genotype incompatibilities in linkage analysis. Am J Hum Genet 63:259–266

Reipert S, Steinbock F, Fischer I, Bittner RE, Zeold A, Wiche G (1999) Association of mitochondria with plectin and desmin intermediate filaments in striated muscle. Exp Cell Res 252: 479–491

Rogalski TM, Mullen GP, Gilbert MM, Williams BD, Moerman DG (2000) The *UNC-112* gene in *Caenorhabditis elegans* encodes a novel component of cell–matrix adhesion structures required for integrin localization in the muscle cell membrane. J Cell Biol 150:253–264

Senturk N, Usubutun A, Sahin S, Bukulmez G, Erkek E, Topaloglu R, Akan T (1999) Kindler syndrome: absence of definite ultrastructural feature. J Am Acad Dermatol 40:335–337

Shimizu H, Sato M, Ban M, Kitajima Y, Ishizaki S, Harada T, Bruckner-Tuderman L, Fine JD, Burgeson R, Kon A, McGrath JA, Christiano AM, Uitto J, Nishikawa T (1997) Immunohistochemical, ultrastructural, and molecular features of Kindler syndrome distinguish it from dystrophic epidermolysis bullosa. Arch Dermatol 133:1111–1117

Smith FJD (2003) The molecular genetics of keratin disorders. Am J Clin Dermatol 4:347–364

Smith FJD, Eady RAJ, Leigh IM, McMillan JR, Rugg EL,

Kelsell DP, Bryant SP, Spurr NK, Geddes JF, Kirtschig G, Milana G, de Bono AG, Owaribe K, Wiche G, Pulkkinen L, Uitto J, McLean WHI, Lane EB (1996) Plectin deficiency results in muscular dystrophy with epidermolysis bullosa. Nat Genet 13:450–457

Sobel E, Lange K (1996) Descent graphs in pedigree analysis: applications to haplotyping, location scores, and marker-sharing statistics. Am J Hum Genet 58:1323–1337

Suga Y, Tsuboi R, Hashimoto Y, Yaguchi H, Ogawa H (2000) A Japanese case of Kindler syndrome. Int J Dermatol 39: 284–286

Weber JL, May PE (1989) Abundant class of human DNA polymorphisms which can be typed using the polymerase chain reaction. Am J Hum Genet 44:388–396

Wick M, Bürger C, Brüsselbach S, Lucibello FC, Müller R (1994) Identification of serum-inducible genes: different patterns of gene regulation during $G_0 \rightarrow S$ and $G_1 \rightarrow S$ progression. J Cell Sci 107 Pt 1:227–239 (erratum 107[Pt 3]:precedi)

Wiebe CB, Silver JG, Larjava HS (1996) Early-onset periodontitis associated with Weary-Kindler syndrome: a case report. J Periodontol 67:1004–1010

Zamir E, Geiger B (2001*a*) Components of cell-matrix adhesions. J Cell Sci 114:3577–3579

——— (2001*b*) Molecular complexity and dynamics of cell-matrix adhesions. J Cell Sci 114:3583–3590

Zhang Y, Flejter WL, Barcroft CL, Riviere M, Szpirer J, Szpirer C, Bina M (1995) Localization of the human HTF4 transcription factors 4 gene (TCF12) to chromosome 15q21. Cytogenet Cell Genet 68:235–238

Zipkin ID, Kindt RM, Kenyon CJ (1997) Role of a new Rho family member in cell migration and axon guidance in C. elegans. Cell 90:883–894